Hydrol. Earth Syst. Sci., 16, 2605–2616, 2012
www.hydrol-earth-syst-sci.net/16/2605/2012/
doi:10.5194/hess-16-2605-2012

Hydrology and Earth System Sciences

Partitioning of evaporation into transpiration, soil evaporation and interception: a comparison between isotope measurements and a HYDRUS-1D model

S. J. Sutanto[1,3,*], **J. Wenninger**[1,2], **A. M. J. Coenders-Gerrits**[2], **and S. Uhlenbrook**[1,2]

[1]UNESCO-IHE, Department of Water Engineering, P.O. Box 3015, 2601 DA, Delft, The Netherlands
[2]Delft University of Technology, Water Resources Section, P.O. Box 5048, 2600 GA, Delft, The Netherlands
[3]Research Center for Water Resources, Ministry of Public Works, Jl. Ir. H. Djuanda 193, Bandung 40135, Indonesia
[*]now at: Institute for Marine and Atmospheric Research Utrecht (IMAU), University of Utrecht, Princetonplein 5, 3584 CC, Utrecht, The Netherlands

Correspondence to: S. J. Sutanto (s.j.sutanto@uu.nl)

Received: 8 March 2012 – Published in Hydrol. Earth Syst. Sci. Discuss.: 16 March 2012
Revised: 20 July 2012 – Accepted: 21 July 2012 – Published: 10 August 2012

Abstract. Knowledge of the water fluxes within the soil-vegetation-atmosphere system is crucial to improve water use efficiency in irrigated land. Many studies have tried to quantify these fluxes, but they encountered difficulties in quantifying the relative contribution of evaporation and transpiration. In this study, we compared three different methods to estimate evaporation fluxes during simulated summer conditions in a grass-covered lysimeter in the laboratory. Only two of these methods can be used to partition total evaporation into transpiration, soil evaporation and interception. A water balance calculation (whereby rainfall, soil moisture and percolation were measured) was used for comparison as a benchmark. A HYDRUS-1D model and isotope measurements were used for the partitioning of total evaporation. The isotope mass balance method partitions total evaporation of $3.4\,\mathrm{mm\,d^{-1}}$ into $0.4\,\mathrm{mm\,d^{-1}}$ for soil evaporation, $0.3\,\mathrm{mm\,d^{-1}}$ for interception and $2.6\,\mathrm{mm\,d^{-1}}$ for transpiration, while the HYDRUS-1D partitions total evaporation of $3.7\,\mathrm{mm\,d^{-1}}$ into $1\,\mathrm{mm\,d^{-1}}$ for soil evaporation, $0.3\,\mathrm{mm\,d^{-1}}$ for interception and $2.3\,\mathrm{mm\,d^{-1}}$ for transpiration. From the comparison, we concluded that the isotope mass balance is better for low temporal resolution analysis than the HYDRUS-1D. On the other hand, HYDRUS-1D is better for high temporal resolution analysis than the isotope mass balance.

1 Introduction

The Food and Agriculture Organization (FAO) and the United Nations World Food Program (WFP) in Rome stated in September 2010 that 925 million people in the world suffer from chronic hunger. People depend on plants for food, and the major environmental factor limiting plant growth is water (Kirkham, 2005). Agriculture needs a huge amount of water, and in the future the amount of water needed for irrigation will increase dramatically due to the increasing population. Best practice agriculture, defined as the agriculture that optimizes water use, is a key to overcome this problem through the improvement of water use efficiency. Thus, most of the water is not lost (e.g. evaporated back to the atmosphere, lost by drainage, deep percolation and surface runoff) but completely used by plants to produce biomass. Therefore, knowledge of the water fluxes within the soil-vegetation system to maximize the productive water loss (transpiration) and minimize the non-productive water loss is crucial. Many studies have been carried out to quantify these fluxes by plants, but they encounter difficulties in quantifying the relative contribution of soil evaporation (E_s) and transpiration (E_t) from total evaporation (E) (Zhang et al., 2010).

The use of environmental isotopes (^{18}O and ^{2}H) with their unique attributes presents a new and important technique to trace fluxes within the soil-plant-atmosphere continuum system (Kendall and McDonnell, 1998; Mook, 2000; Wenninger et al., 2010; Zhang et al., 2010). The reason for using

these tracers is that they are chemically and biologically stable and show no isotopic fractionation during water uptake by roots (Ehleringer and Dawson, 1992; Kendall and McDonnell, 1998; Tang and Feng, 2001; Yepez et al., 2003; Williams et al., 2004; Balazs et al., 2006; Koeniger et al., 2010). Moreover, partition of the evaporation fluxes using isotopes has many advantages compared with other methods such as lysimeter measurements, sapflow measurements, remote sensing information, and micrometeorological techniques, since these methods have several limitations (Xu et al., 2008; Rothfuss et al., 2010).

An earlier study where evaporation was measured with deuterium was carried out by Calder et al. (1986) and Calder (1992) in India; however, they had only measured the transpiration flux. In the last decade, partitioning of total evaporation into soil evaporation and transpiration using stable isotopes was studied by Yepez et al. (2003, 2005); Williams et al. (2004); Robertson and Gazis (2006); Xu et al. (2008); Rothfuss et al. (2010); Wang et al. (2010, 2012a); Wenninger et al. (2010); Zhang et al. (2010, 2011). Williams et al. (2004) used the combination of eddy covariance, sapflow, and stable isotope measurements in an irrigated olive orchard, in Morocco.Yepez et al. (2003, 2005) separated the evaporation flux into soil evaporation and transpiration and estimated the ratio of transpiration from total evaporation using Keeling plots of water vapor under transient conditions. Xu et al. (2008) partitioned soil evaporation and transpiration using a combination of Keeling plots and stable isotopes. Some methods to partition total evaporation are explained by Zhang et al. (2010), such as the mass balance approach, Craig-Gordon formulation, Keeling plot method, and flux-gradient method. Wang et al. (2010) partitioned evaporation based on a combination of a newly developed laser-based isotope analyzer and the Keeling plot approach. An isotope mass balance method has been used to partition evaporation into soil evaporation and transpiration and is useful to estimate the contribution of evaporation and transpiration during different hydrologic seasons (Ferretti et al., 2003; Robertson and Gazis, 2006; Wenninger et al., 2010). Zhang et al. (2011) partitioned evaporation into soil evaporation and transpiration using a combined isotopic and micrometeorologic approach. The latest technique to quantify the transpiration flux was introduced by Wang et al. (2012a). They used the mass balance method of both water vapor and water vapor isotopes inside a chamber. Moreover, Wang et al. (2012b) present a detailed discussion of isotope-based evaporation partition in their new paper.

All these studies tried to partition the evaporation fluxes into soil evaporation and transpiration flux only, without taking into account the interception flux. The interception flux can be an important component in the evaporation process and should not be neglected (Savenije, 2004; Gerrits et al., 2009, 2010). Moreover, partitioning with and without taking into account the interception flux will give different portions of soil evaporation and transpiration. Hence, in this study in contrast to others, we report the partitioning of evaporation into soil evaporation and transpiration under consideration of interception using a combination of hydrometric measurements and stable isotopes. It should be noted that we did not measure interception directly but we modeled the interception flux based on known interception threshold value from the past study conducted by Gerrits (2010). The other advantages of this study are that a widely available liquid water isotope analyzer and non-expensive hydrometric measurement devices were used. Meanwhile, most of the other studies used more equipment to measure the isotopic composition of transpiration flux in stem water, water vapor, ground water, etc.

2 Materials and methods

2.1 Experimental set-up

A grass-covered lysimeter was installed in the laboratory of UNESCO-IHE, the Netherlands. The set-up consists of a weighing lysimeter made from a PVC tube with five soil moisture sensors (Decagon 5TE ECH2O probes) and five Rhizon soil moisture samplers (10 cm porous, OD 2.5 mm, sswire, 12 cm tubing) attached to it (Fig. 1). The lysimeter has a length of 40 cm and a diameter of 20 cm and contains soil taken from a grass area in the Botanical Garden of Delft University of Technology, the Netherlands. The soil sample was collected according to the following procedure: (I) the PVC tube was forced into the grass-soil until the PVC tube was completely filled with soil and grass. (II) After filling, the PVC tube was taken out and sealed at the bottom part. (III) In the laboratory, the PVC tube was installed on top of the percolation device and then equipped with the soil moisture sensors and Rhizon samplers. (IV) The gap between the PVC tube and percolation device was glued to prevent evaporation from the contact interface of the lysimeter and percolation device.

A wet sieving analysis was carried out to determine the soil types of soil column. The particle distribution used for the wet sieving analysis comprises the following: gravel with a diameter more than 2 mm; sand between 63 µm and 2 mm; coarse silt between 38 µm and 63 µm; medium and fine silt and clay less than 38 µm. The results from the wet sieving analysis show that the lysimeter contains gravel, sand, silty clay and clay materials. The dominant fractions in the top layer are sand (77 %), clay (16.4 %) and a small amount of gravel and silt, whereas, the middle layer is composed of gravel (25.6 %), sand (47.5 %), clay (22.5 %) and silt (4.3 %), and the bottom layer of sand (62.7 %), clay (27.4 %) and silt and gravel for the rest percentage.

Five soil moisture sensors with an electromagnetic field to measure the dielectric permittivity of the surrounding medium were horizontally pushed into the undisturbed soil to monitor the soil moisture, bulk electrical conductivity (EC), and soil temperature. The temperature was measured using

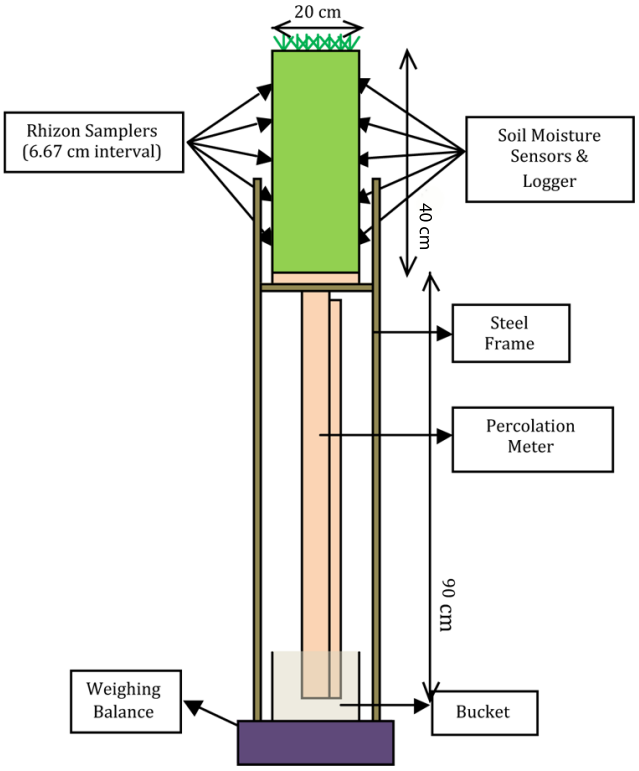

Fig. 1. Schematic sketch of the experimental set-up.

a surface-mounted thermistor located underneath the probe and reading the temperature of the prong surface. EC was measured by applying an alternating electrical current to two electrodes measuring the resistance between them. The accuracy of the 5TE ECH2O probes is 0.08 % for soil moisture, 0.05 dS m^{-1} for EC and 0.1 °C for temperature. The Rhizon soil moisture samplers were installed in the opposite direction of the soil moisture sensors to prevent rapid soil moisture changing due to abstraction of water. The Rhizon samplers are made from a thin hose with a porous filter (0.15–0.2 µm) on top and a connector to attach the syringe at the bottom. The distance interval between two soil moisture sensors as well as the Rhizon samplers was 6.67 cm. The bottom of the lysimeter was filled with drainage material (diatomaceous earth with diameter of 10 to 200 µm) to enhance the contact between the lysimeter and percolation device.

Percolation was measured using a Decagon drain gauge G2 (passive-wick system) placed underneath the intact soil monolith. This drain device has a 150 ml reservoir, ±0.1 mm resolution and 10 ms measurement time. The passive-wick system has some limitations, in that there can be a mismatch between the soil water suction and that applied to the wick by the length of the hanging water column (Meissner et al., 2010). However, the differences may be relatively small, especially for sandy soil. Decagon EM50 data loggers with one-minute measurement interval were used to store the data. This set-up was mounted on a Kern DE60K20N platform balance to measure the water losses inside the lysimeter. This device has a maximum weighing range of 60 kg and readability of 20 g. A bucket was placed under the percolation device to store excess water, if the percolated water overflows the percolation device due to the storage limitation. The experiments were carried out from 16 November 2010 until 31 January 2011.

To simulate rainfall, tap water was sprinkled uniformly on the lysimeter with a bucket. The bottom of the bucket perforated with small holes (less than 1 mm diameter) let the water out from the bucket as sprinkled precipitation. The temporal precipitation pattern applied in the laboratory was designed based on the average summer precipitation pattern of a nearby KNMI (*Koninklijk Nederlands Meteorologisch Instituut*) weather station in Rotterdam for June and July from 2005 to 2010 and was applied in November and December 2010, respectively. In January 2011, the precipitation was sprinkled every 3 to 5 days. The accuracy of precipitation sprinkling was around 2 ml.

A weather station (Catec Clima Sensor 2000 type 4.9010.00.061) using a Grant Squirrel data logger was installed in the laboratory to measure relative humidity, temperature, wind speed, and solar radiation. The accuracy of the sensors of the weather station is 10 % for the pyranometer, $< 0.5\,m\,s^{-1}$ for wind speed, 0.15 °C for temperature and 3 % for relative humidity. The height difference between measurement devices and lysimeter surface is 15–20 cm.

One lamp (OSRAM powerstar 400 W) was installed above the lysimeter to compensate for the sunlight inside the laboratory. Timers were used to control the lamp and fan. The lamp was switched on at 6 a.m. and switched off at 6 p.m. The fan was turned on at 6 a.m. and turned off at 5 p.m. The value ranges of radiation, wind speed, temperature and humidity are 1–31 W m^{-2}, 0–1.2 m s^{-1}, 18–29 °C and 18–45 %, respectively. Evaporation data from the Rotterdam station were used for comparison. Average evaporation calculated with Makkink formula for Rotterdam during summer period (2005 to 2010) was 2.5–3.5 mm d^{-1}. Daily meteorological measurements and precipitation in the laboratory are presented in Fig. 2.

2.2 Isotope analysis

2.2.1 Isotope measurements

The isotope measurements were carried out bi-weekly at the beginning of the experiment and more frequently towards the end of the experiment (e.g. in January). Soil water was abstracted from every layer in the lysimeter with Rhizon soil moisture samplers by applying a vacuum with 30 ml syringes for the isotope analysis. Water samples were analyzed with the LGR liquid water isotope analyzer (LWIA-24d). The analyzer measures ^{18}O and ^{2}H in liquid water samples with high accuracy (±0.2 ‰ and ±0.6 ‰, respectively) in a sample

volume of $< 10\,\mu l$. The results are reported in δ values, representing deviations in per-mil (‰) from the Vienna Standard Mean Ocean Water (VSMOW):

$$\delta = \frac{R_{\text{sample}}}{R_{\text{VSMOV}}} - 1 \quad (1)$$

where R_{sample} is the isotopic abundance ratio of, for example, $^2H/H_2O$ in the sample and R_{VSMOV} is the isotopic abundance ratio of the Vienna Standard Mean Ocean Water. It is convenient and common to multiply the δ values by 1000 as ‰ difference from the standard being used.

2.2.2 Equilibrium and kinetic fractionation

The fractionation process changes the isotopic composition. Equilibrium fractionation occurs from the transformation of water phase such as evaporation, melting, condensation, freezing, sublimation. This fractionation between two substances can be expressed by the isotope fractionation factor α:

$$\alpha_{\text{A-B}} = \frac{R_{\text{t}}\text{A}}{R_{\text{B}}} \quad (2)$$

where R is the ratio of the two phases A (e.g. water) and B (e.g. vapor). The equilibrium enrichment factor $\varepsilon_{\text{eq(A-B)}}$ is also expressed in ‰ :

$$\varepsilon_{\text{eq(A-B)}} = \left(\frac{R_{\text{A}}}{R_{\text{B}}} - 1\right) \cdot 1000\ ‰ = (\alpha_{\text{A-B}} - 1) \cdot 1000\ ‰. \quad (3)$$

The fractionation factor is commonly expressed as "$10^3 \ln\alpha$" because this expression is very close to the per mil fractionation between the materials and is nearly proportional to the inverse of temperature ($1/T$) at low temperatures in kelvin (Kendall and McDonnell, 1998). Szapiro and Steckel (1967) and Majoube (1971), as cited in Clark and Fritz (1997), give the following equation to quantify the equilibrium fractionation factor from liquid (A) to vapor phase (B):

$$10^3 \ln\alpha_{\text{A-B}} = \frac{10^6 a}{T^2} + \frac{10^3 b}{T} + c. \quad (4)$$

T is temperature in kelvin; constants a, b and c for ^{18}O are $a = 1.137$, $b = -0.4156$, and $c = -2.0667$ and $a = 24.844$, $b = -76.248$ and $c = 52.612$ for ^2H.

The other fractionation process is the kinetic fractionation (ε_k) which is a process that separates stable isotopes from each other by their mass during un-idirectional processes. The factors that affect kinetic fractionation of water during the evaporation process are humidity, salinity and temperature. The effect of humidity on isotope enrichment can be expressed as follows (h is humidity, %) (Clark and Fritz, 1997):

$$\varepsilon_{k(\text{A-B})} = 10^3 \ln\alpha^{18}\text{O}_{\text{A-B}} = 14.2(1-h)‰ \quad (5)$$

$$\varepsilon_{k(\text{A-B})} = 10^3 \ln\alpha^{2}\text{H}_{\text{A-B}} = 12.5(1-h)‰ \quad (6)$$

The overall fractionation by evaporation is the sum of equilibrium and kinetic fractionation ($\varepsilon_{\text{total}} = \varepsilon_{\text{eq}} + \varepsilon_k$) (Dongmann et al., 1974).

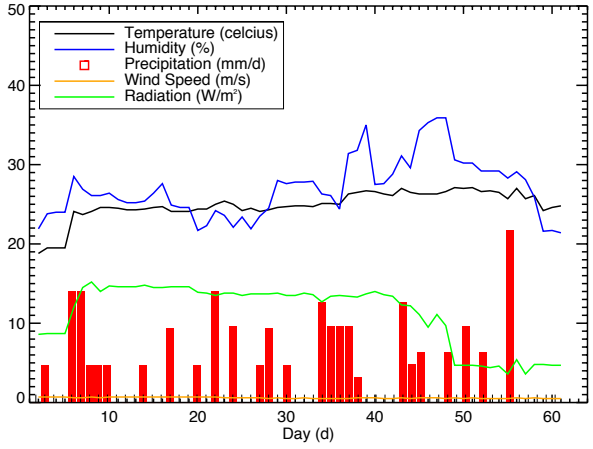

Fig. 2. Daily meteorological measurements and applied precipitation in UNESCO-IHE laboratory for December and January.

2.3 Interception

Interception is the part of rainfall that is intercepted by the Earth's surface such as vegetation, soil surface, litter, rock, roads, etc (Sutanudjaja et al., 2011; Gerrits, 2010; Savenije, 2004). Interception can be defined as a stock (S), flux or the entire interception process (Gerrits et al., 2007, 2010). The stock refers to the amount of water that grass can store (i.e. the storage capacity), and the flux refers to the successive evaporation from this storage. Interception models like a Rutter-like model also use this threshold value (S) (Rutter et al., 1971). Gerrits (2010) measured for a grassland area in Westerbork (the Netherlands) a storage capacity of 2 mm. Both the isotope mass balance calculation and the HYDRUS-1D model use the interception flux; thus, the stock values (mm) need to be converted into flux values (mm d^{-1}) by multiplying the stock value by the mean number of precipitation events per day to get the daily interception threshold (Gerrits et al., 2009). In this case, we have 30 rainfall events in 77 days. This results in a daily interception threshold, D of $1\,\text{mm d}^{-1}$. This threshold is used as interception value for both the isotope mass balance method and the HYDRUS-1D model.

This threshold was used to calculate the net precipitation in the isotope mass balance model (Eq. 7). We assume that the net precipitation that infiltrates into the soil is not affected by isotope fractionation. A study from Gehrels et al. (1998) also showed that interception will not play a significant role in isotope fractionation for lower vegetation types. Thus, the net precipitation has the same isotope signature as precipitation. The isotope mass balance calculation using the net precipitation will only give the soil evaporation and transpiration fluxes. Therefore, interception was calculated from the differences of the evaporation flux with and without using the net precipitation.

For the HYDRUS-1D model, interception is (pre-) programmed in a different way (Eq. 8), where a daily interception threshold D [mm d^{-1}] is required. D can be estimated by multiplying S by the number of rainfall events per day. In this way, we found $D = 1$ mm d^{-1}. Since we did not have some parameters, we calibrated the parameters a of the interception module in such way that D equals 1 mm d^{-1} (see Eq. 8). LAI (Leaf Area Index) used in this analysis is LAI for clipped grass (crop height $h_c = 0.05$–0.15 m). Constant b is the surface cover fraction, which is defined in Eq. 10. Details of these formulas can be found in the HYDRUS-1D manual version 4 (Simunek et al., 2008). The interception formula from the net precipitation and the HYDRUS model are described as follows:

$$P_{\text{net}} = \max(P - D, 0) \tag{7}$$

$$D = a \cdot \text{LAI}\left(1 - \frac{1}{1 + \frac{bP}{a \cdot \text{LAI}}}\right) \tag{8}$$

$$\text{LAI} = 0.24 \cdot h_{\text{grass}} \tag{9}$$

$$b = 1 - \exp(-k \cdot \text{LAI}) \tag{10}$$

where D is the daily interception threshold [L T^{-1}], h_{grass} the grass height, k is rExtinct = 0.463, LAI the leaf area index [L L^{-1}], P precipitation [L T^{-1}], and a the constant entered from the HYDRUS-1D interface (we found 4.5 mm).

2.4 Evaporation analysis

2.4.1 Water balance

With this method, evaporation is calculated based on the differences between precipitation, storage changes, and percolation. The weighing balance measures the storage changes in the lysimeter directly. The water balance formula is described as a follows:

$$\frac{\mathrm{d}S}{\mathrm{d}t} = P - E_a - L = P - E_s - E_t - E_i - L \tag{11}$$

where P is precipitation [L T^{-1}], E_a total evaporation [L T^{-1}] ($E_a = E_s + E_t + E_i$), L percolation [L T^{-1}], $\mathrm{d}S/\mathrm{d}t$ changes of storage in the soil [L T^{-1}], E_s soil evaporation [L T^{-1}], E_t transpiration [L T^{-1}], and E_i interception [L T^{-1}].

2.4.2 HYDRUS-1D model

The HYDRUS-1D model can be used to simulate the water and solute movement in unsaturated, partly saturated or fully saturated porous media (Simunek et al., 2008). The HYDRUS-1D model for one-dimensional water movement is based on the modified Richards equation with the assumption that the air phase plays an unimportant role in the liquid flow process, and water flow due to thermal gradients can be neglected.

$$\frac{\mathrm{d}\theta}{\mathrm{d}t} = \frac{\mathrm{d}}{\mathrm{d}x}\left[K\left(\frac{\mathrm{d}h}{\mathrm{d}x} + \cos\alpha\right)\right] - S \tag{12}$$

where θ is volumetric soil water content [L^3 L^{-3}], t time [T], h the soil water pressure head [L], x the spatial coordinate [L], K unsaturated hydraulic conductivity [L T^{-1}], α angle between the flow direction and vertical axis ($\alpha = 0°$ for vertical flow, $\alpha = 90°$ for horizontal flow), and S the sink term [L^3 L^{-3} T^{-1}].

The sink term (S), defined as the volume of water removed from the soil per unit of time due to plant water uptake, can be described as

$$S(h) = \alpha(h) S_p \tag{13}$$

where S_p is the potential water uptake rate [T^{-1}] and $\alpha(h)$ the given dimensionless function of the soil water pressure head ($0 \le \alpha \le 1$). The term $\alpha(h)$ was defined as a functional form by Feddes et al. (1974, 1978). The HYDRUS-1D model calculated the transpiration flux based on water uptake distribution with some assumptions: water uptake is assumed to be zero if it is close to saturation and in the wilting point pressure head; water uptake is optimal when $\alpha(h)$ is equal to 1, which means water uptake is maximal, and stress condition is occurring due to dry or wet condition and high salinity (Feddes et al., 1978; Genuchten, 1987; Feddes et al., 2001; Simunek et al., 2008).

In the HYDRUS-1D, potential evaporation is calculated using either Penman-Monteith or Hargreaves formula. Beer's law method is used to partition potential transpiration and soil evaporation fluxes as follows:

$$E_t = E \cdot \text{SCF} \tag{14}$$

$$E_s = E \cdot (1 - \text{SCF}) \tag{15}$$

where E_t is potential plant transpiration, E_s is potential soil evaporation and SCF is the soil cover fraction defined as constant b in Eq. (10). Thus, this potential evaporation is used as an input to calculate the actual evaporation fluxes based on Feddes reduction for transpiration and hCritA limit for soil evaporation (Simunek et al., 2008).

In this study, the HYDRUS-1D modeling has been divided into three parts. The first part is the calibration process to obtain the soil parameters. The model was calibrated on the observed soil moisture data by inverse modeling. The second part is the validation process, and the last part is the complete simulation from November to January. Calibration and validation were carried out from the first to the end of December and the first of January until the end of January, respectively.

We schematized our soil column as two soil layers top and bottom which are influenced most by evaporation and percolation. The top layer (0–6.67 cm) consists of sand, whereas the bottom layer (33.3–40 cm) of clay-silt. Default soil parameters from the HYDRUS-1D soil database were used as

starting parameters. Root depth was observed at 5 cm. Hence in the model, the root distribution value of one was used for the surface, which decreased to zero in the depth more than 5 cm. Initial soil moisture was obtained from the soil moisture sensors, which was 0.22 ($m^3\,m^{-3}$) for the surface layer to 0.38 ($m^3\,m^{-3}$) at the bottom. The Feddes root water uptake model was chosen to simulate the amount of water taken up from the soil for transpiration using the default parameters for grass (Feddes et al., 1974, 2001).

The soil parameters include Θ_r for the residual water content, Θ_s the saturated water content, α and n parameters describing the shape of soil water retention curve and hydraulic conductivity curve, K_s the saturated hydraulic conductivity and I the pore-conductivity, and they were calibrated using inverse modeling. This inverse modeling estimates the calibrated parameters by fitting the observed and the modeled soil moisture based on Marquardt-Levenberg optimization algorithm. In this model, soil hydraulic properties are assumed to be described by an analytical model. HYDRUS produces a correlation matrix which specifies the degree of correlation between the fitted coefficients and runs the optimization process until it finds the highest R^2 values (Simunek et al., 2008). The time step used in this model is one hour with the length unit in mm. The single porosity van Genuchten-Mualem model was used for the soil hydraulic model simulation without hysteresis. The boundary conditions used in this model are the atmospheric boundary condition for the upper boundary and a free drainage for the bottom boundary. See Simunek et al. (2008) for more detailed information regarding the HYDRUS-1D theory, method and default parameters.

2.4.3 Isotope mass balance calculation

The isotope mass balance calculation has been carried out to calculate the amount of water used for soil evaporation and transpiration. The assumption used in this calculation is that the water taken by plant roots for transpiration is not affected by isotope fractionation until the water is leaving the plant via the stomata (Ehleringer and Dawson, 1992; Kendall and McDonnell, 1998; Tang and Feng, 2001; Riley et al., 2002; Williams et al., 2004; Balazs et al., 2006; Gat, 2010). In contrast, the evaporated water from the soil and interception are affected by isotope fractionation. Therefore, interception needs to be subtracted from the precipitation in order to get the net precipitation, which is assumed to have the same isotopic composition as the precipitation. The net precipitation is not mixed with the (partly) fractionated interception water on the grass surface. Hence, in the isotope mass balance calculation, the net precipitation values were used. The isotope mass balance can be formulated as

$$m_i + m_p = m_e + m_f + m_t + m_l = m_{total} \tag{16}$$

and

$$\delta_i x_i + \delta_p x_p = \delta_e x_e + \delta_f x_f + \delta_t x_t + \delta_l x_l \tag{17}$$

where m_i [M] is the initial mass, m_p [M] net precipitation mass, m_e [M] evaporation mass, m_f [M] final mass, m_t [M] transpiration mass, and m_l [M] percolation mass. δ represents, for example, the $\delta^{18}O$ (per mil) of each component and x the fraction of water in the respective component. Thus, δ_i is $\delta^{18}O$ for the initial measurement, δ_p is $\delta^{18}O$ for the net precipitation, δ_e is $\delta^{18}O$ for evaporation, δ_f is $\delta^{18}O$ for final measurement, δ_t is $\delta^{18}O$ for transpiration, and δ_l is $\delta^{18}O$ for percolation. m_{total} is calculated from the initial soil water mass and precipitation mass ($m_{total} = m_i + m_p$), and the fraction of each component (j) is calculated as $x_j = m_j / m_{total}$. δ_i and δ_f are the initial and final isotope values in the soil water calculated using weighted average of isotopic composition in every layer.

$$\delta_i = \delta_f = \frac{\sum_{j=1}^{n}(\delta_{sj} \cdot H_j \cdot SWC_j)}{\overline{SWC}} \cdot H_{total} \tag{18}$$

where n is number of layer, δ_{si} is the δ value in the soil layer i, H_i is a correspondence depth of layer i, SCW_i is the soil water content in layer i, $\overline{SWC}$ is average of soil water content and H_{total} is total depth.

The isotopic contents of transpired water and deep percolated water are not affected by isotopic fractionation and these terms can be combined as non-fractionation terms (x_{nf}). Moreover, the isotopic content of this water is equal to the average δ value of soil water over time interval δ_i and δ_f (Robertson and Gazis, 2006). δ_e can be calculated from δ_t minus total isotope fractionation (ε_{total}):

$$\delta_{nf} = \delta_t = \delta_l \tag{19}$$

$$\delta_t = \delta_l = \frac{(\delta_i + \delta_f)}{2} \tag{20}$$

$$\delta_e = \delta_t - \varepsilon_{total} \tag{21}$$

$$x_{nf} = x_p + x_i - x_e - x_f \tag{22}$$

$$x_t = x_{nf} - x_l \tag{23}$$

Evaporated water (x_e) as an unknown variable can be calculated based on the derivation of Eq. (17) and substitutes it with Eq. (19) to Eq. (23). The final product from the derivation is Eq. (24) where there is no unknown parameter in the equation.

$$x_e = \frac{x_i\delta_i + x_p\delta_p - x_f\delta_f - x_p\delta_{nf} + x_f\delta_{nf} - x_i\delta_{nf}}{\delta_e - \delta_{nf}} \tag{24}$$

3 Results and discussion

3.1 Soil water content and HYDRUS-1D modeling

The result from the soil water content measurements for depth 6.7, 20 and 33.3 cm is illustrated in Fig. 3. The fluctuation of soil moisture is strongly influenced by rainfall. The

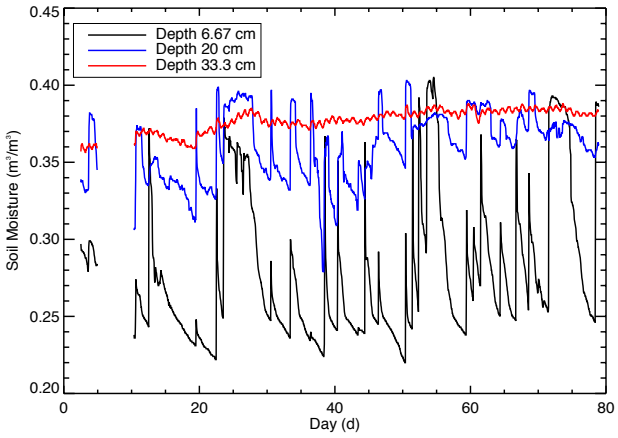

Fig. 3. Soil moisture data measured in the lysimeter from 16 November to 31 January (depth 13.3 and 26.6 cm results are not plotted in order to make a readable graph).

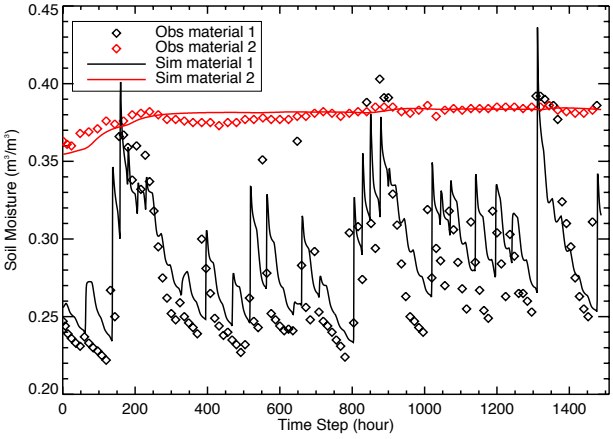

Fig. 4. HYDRUS-1D calibration results (in December, time step 0–744); HYDRUS-1D validation results (in January, time step 745–1488).

sensors in the upper part are mostly affected by precipitation. Depth 6.7 cm from surface showed indeed a quick response to precipitation. In contrast, depth 33.3 cm from the surface showed a less distinct response to precipitation water. The fast response at depth 6.6 cm can be caused by macropores in the soil, soil cracking, or flow at the boundary between the soil and PVC pipe.

The HYDRUS-1D model was used to simulate the water fluxes inside the lysimeter. The calibration results for both materials are good with $R^2 = 0.94$. However, the R^2 value is not the best indication for model and data agreement. Table 1 shows the calibrated parameters. After calibration, the calibrated parameters were used to simulate the data in January to validate the model. The validation results are acceptable, although the R^2 value is 0.82. The calibration and validation results starting from December to January simulation are presented in Fig. 4 and the calibrated parameters in Table 1.

Figure 4 shows that the simulation results for material 1 are unable to capture some peak values, although the recession limbs from the model fit the observations. However, material 2 shows that the observed values and simulated values agree well. In addition, percolation can also be used for model calibration. Total modeled percolation in December 2010 is 0.1 mm/month, while the observed percolation was 0.4 mm/month. However, total percolation during the entire measurement period (3 months) is 2.4 mm and total percolation simulated by the HYDRUS-1D model was only 0.35 mm.

Although the total observed percolation is 2.4 mm and total modeled percolation 0.35 mm, the percolation result from the model is still acceptable. The percolation error is 2.05 mm in 2.5 months or less than 1 mm per month. The difference between model results and observations may be caused by macro-pores, roots, soil cracking, etc. HYDRUS-1D assumes a perfect homogenous soil column while, in fact, the soil column may contain those causative factors.

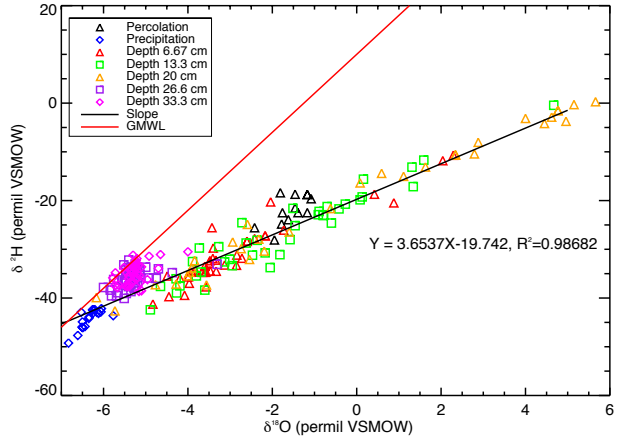

Fig. 5. Isotope measurement results plotted against GMWL.

3.2 Isotopic composition of soil water

The isotopic composition of soil water is shown in Fig. 5. As expected, the isotope results show that the water inside the lysimeter is affected by evaporation in non-equilibrium processes which is indicated by a slope less than 8 for the evaporation line (Dansgaard, 1964). The overall evaporation line has a slope of 3.6 and an intercept value of −19.7 ‰ ($R^2 = 0.99$). The soil water at depth (z) 6.6 cm has an evaporation slope of 3.9 and an intercept value of −19.6 ‰. For $z = 13.3$ cm, the line has a slope of 3.8 and an intercept of −20.2 ‰, and for $z = 20$ cm, an evaporation slope of 3.6 and an intercept value of −19.7 ‰. These slope values are comparable with other studies in vadose zones that

Table 1. The calibrated parameters from HYDRUS-1D inverse modeling (Θ_r is the residual water content, Θ_s saturated water content, α and n parameters describing the shape of soil water retention curve and hydraulic conductivity curve, K_s saturated hydraulic conductivity and I pore-conductivity).

Name	Θ_r ($cm^3\,cm^{-3}$)	Θ_s ($cm^3\,cm^{-3}$)	α (1/cm)	n (–)	K_s ($cm\,d^{-1}$)	I ($cm\,cm^{-1}$)
Material 1	0.12960	0.50069	0.00152	1.76900	4.53730	0.34815
Material 2	0.17852	0.39118	0.00077	1.05420	0.32555	0.55768

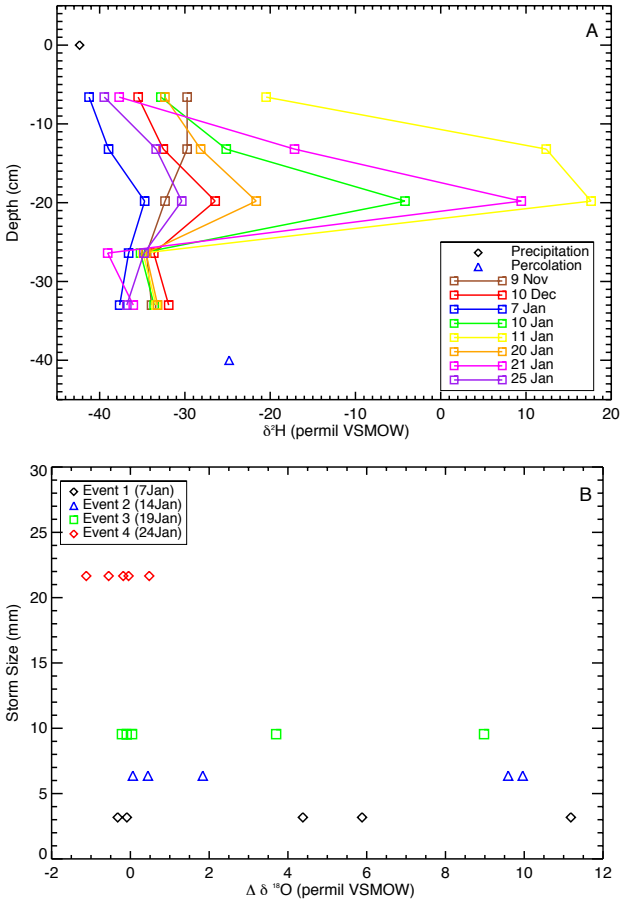

Fig. 6. Several isotopes profiles in the lysimeter measured during study period (A); $\Delta\ ^{18}O$ in several precipitation events (B).

have evaporation slopes between 2 to 5 (Allison, 1982; Clark and Fritz, 1997; Kendall and McDonnell, 1998; Wenninger et al., 2010). The evaporation line shows that the kinetic enrichment of ^{18}O in the evaporating water is more than the enrichment in ^{2}H. The water in the upper part of the lysimeter has, as expected, higher soil evaporation rates compared to the water in the lower part of the soil. Precipitation, soil moisture at $z = 33.3$ cm, and some of the samples at $z = 26.6$ cm are laying on the GMWL. This means that evaporation has little effect on the bottom part of the lysimeter.

For a better overview of the isotope fractionation, the isotope values are plotted against depth and time (see Fig. 6a). High values of ^{2}H and ^{18}O appear at depths of 6.6, 13.3, and 20 cm, and the highest value occurs at a depth of 20 cm from the soil surface. It shows that the effect of evaporation occurs from the surface until 20 cm depth and the maximum value at 20 cm depth is called the drying front. This enrichment is caused by kinetic effects of diffusion (Barnes and Turner, 1998; Clark and Fritz, 1997). Zhang et al. (2011) also show that the evaporation depth is approximately 20 cm. The shape from the surface to 20 cm depth is performed by vapor diffusion, and the shape from below 20 cm depth is caused by downward diffusion of isotopes. The precipitation can push the enriched water downward, but the isotopic composition of soil water after 20 cm will be depleted in heavy isotopes since a downward diffusion process is taking place. Rain water origining from tap water shows an isotopic composition of -40 to -50 ‰ for ^{2}H. Percolation water has an isotope range between -15 to -30 ‰ and is more enriched compared to the isotope value from depth 33.3 cm. This enrichment of isotopes in the percolation water may be caused by the evaporation process inside the percolation meter and mixing water from the top layer, which is isotopically enriched. The percolation meter is not a completely closed device, and there may be a crack inside the lysimeter between the soil column and the PVC pipe.

To analyze the relationship between storm size and enrichment, $\Delta^{18}O$ was plotted per rain event (see Fig. 6b). $\Delta^{18}O$ is the difference between $\delta^{18}O$ from the next sampling ($\delta^{18}O_{t+1}$) minus $\delta^{18}O$ before the rain event ($\delta^{18}O_t$). Figure 6b shows that small precipitation events have more enrichment of $\delta^{18}O$. On the contrary, heavy storm events hardly enrich in their isotopic composition in one day. Storm sizes of 3.2 mm, 6.4 mm, 9.5 mm and 21.6 mm have a maximum $\Delta^{18}O$ in fractionation of 11.2 ‰, 9.9 ‰, 8.9 ‰ and 0.5 ‰, respectively. The greater the storm event is, the smaller the enrichment. On the contrary, the smaller the storm is, the greater the enrichment. This phenomenon may be explained by the mobile and immobile soil water concept. Soil water inside small pores (e.g. clay less than 2 µm diameter) is immobile compared with soil water in large pores (e.g. sand more than 0.3 mm diameter) which is mobile. These small pores have a long water-residence time and can only be replaced with heavy precipitation events (Brooks et al., 2010). Therefore, heavy storms replenish all water inside the soil pores, both mobile and immobile. Thus, the isotopic composition in the soil water is hardly becoming enriched. However,

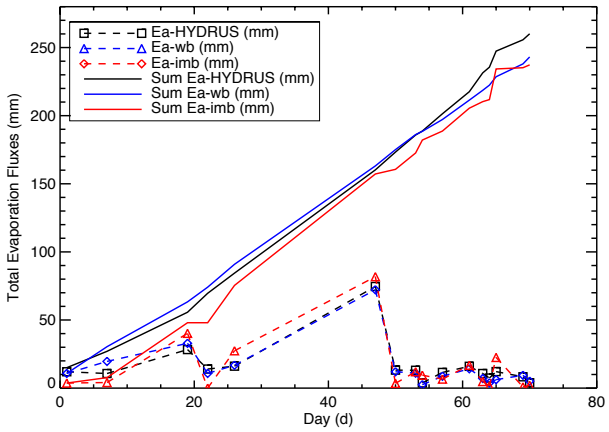

Fig. 7. Comparison of estimated evaporation using three different methods (E_a−HYDRUS evaporation from HYDRUS-1D, E_{a-imb} evaporation from isotope mass balance, E_{a-wb} evaporation from water balance, sum stands for cumulative flux).

small storms only replace the mobile soil water and the Rhizon sampler abstracts the mixing water between mobile and immobile water (which may have a heavily isotopic composition due to evaporation) after several days.

3.3 Evaporation analysis

The evaporation analysis was carried out using the HYDRUS-1D model, the isotope mass balance, and the water balance for comparison. Figure 7 compares the results for these three methods. The straight lines are the cumulative evaporation fluxes, and the dashed lines are the cumulative evaporation fluxes between two isotope samplings. The evaporation fluxes can be analyzed using the isotope mass balance method when there are at least two isotope samples. The first measurement is used as an initial background value, and the second measurement is the final value influenced by the isotope fractionation due to evaporation. The second measurement has evaporation signature between the first and second measurements recorded in isotope value. Thus, the evaporation flux measured in the second measurement is the total evaporation flux from first to second measurements. For example, day 47 has an evaporation value of 81.8 mm. This value is the total evaporation flux between day 26 to day 47. This means that the average evaporation rate during that day is 3.9 mm d^{-1}. The high temporal resolution can be seen at the end of measurement period when more frequent samples were taken.

It is seen from Fig. 7 that the evaporation estimation of the isotope mass balance, the HYDRUS-1D model and the water balance calculation is in good agreement. Actual evaporation calculated with the water balance method is believed to be the most accurate actual evaporation calculation compared to the other methods, since this method uses a weighing balance to measure the losses of water inside the lysimeter directly due to evaporation and percolation. This method was used as a benchmark for the other methods. Table 2 summarizes the evaporation analysis results. The difference between the isotope mass balance method and the water balance is −5.8 mm, while the difference between the HYDRUS-1D model and the water balance is 13.1 mm in 2.3 months. The results show that the isotope mass balance method is better compared to the HYDRUS-1D model to calculate the total evaporation and the average evaporation flux.

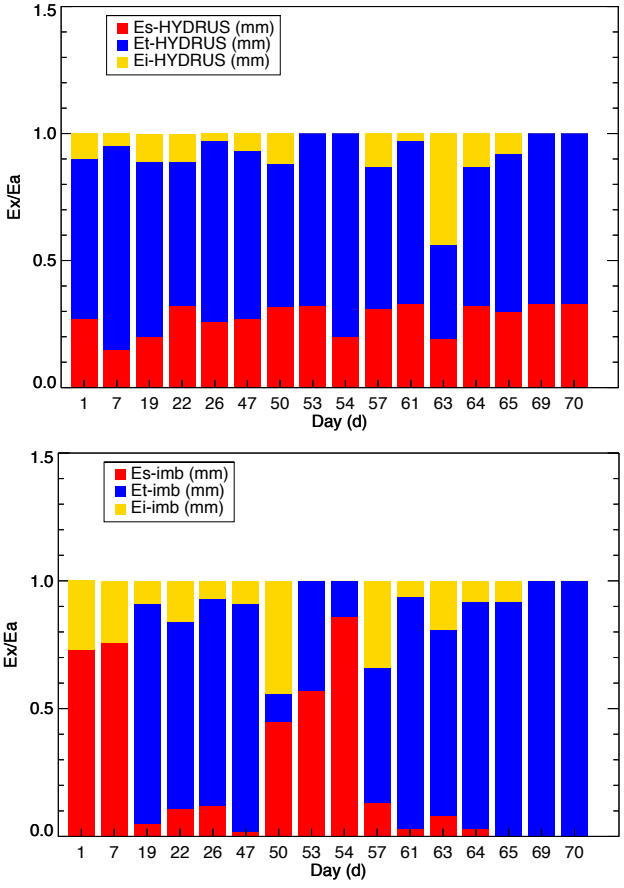

Fig. 8. The ratio of partitioning fluxes compared to total evaporation (E_x/E_a). x stands for soil evaporation, transpiration and interception.

Figure 8 shows the ratio of partitioning fluxes compared to the total evaporation. The ratio of partitioning fluxes from the HYDRUS-1D model is relatively steady compared to the isotope mass balance result. Soil evaporation from the HYDRUS-1D model is more or less 27 % from the total evaporation flux, and the biggest ratio is transpiration flux, which is 64 % while interception is only 10 %. On the other hand, The fluxes ratio from isotope mass balance result is highly fluctuated especially for soil evaporation and transpiration fluxes. In the beginning of the measurements, the total evaporation flux is only partitioned into soil evaporation and

Table 2. Evaporation analysis summary from 16 November 2010 until 27 January 2011. E_a is the total evaporation, E_s soil evaporation, E_t transpiration and E_i interception, while $\overline{E_a}$ is the mean total evaporation, $\overline{E}_s$ mean soil evaporation, $\overline{E}_t$ mean transpiration and $\overline{E}_i$ mean interception.

Methods	E_a (mm)	E_s (mm)	E_t (mm)	E_i (mm)	$\overline{E_a}$ (mm d^{-1})	$\overline{E}_s$ (mm d^{-1})	$\overline{E}_t$ (mm d^{-1})	$\overline{E}_i$ (mm d^{-1})
Water balance	243.1	–	–	–	3.5	–	–	–
HYDRUS-1D	256.2	68.9	164	23.3	3.7	1 (26.9 %)	2.3 (64.1 %)	0.3 (9 %)
Isotope mass balance	237.3	28.8	184.5	24	3.4	0.4 (12.1 %)	2.6 (77.7 %)	0.3 (10.1 %)

interception fluxes. In contrast, in the end of measurements, transpiration flux has the same amount with the total evaporation flux. This is not true since transpiration and soil evaporation fluxes were always produced during evaporation process. This high fluctuation makes the isotope mass balance method less reliable compared to the HYDRUS-1D model for high temporal resolution analysis. The uncertainty of the isotope mass balance method is too high for this temporal resolution. This is due to the fact that the differences in isotope value of certain parts within the soil are too small compared to the accuracy of the measurement. However, the average values of these fluxes during measurement periods compare well between the HYDRUS-1D model and the isotope mass balance method. It should be noted that we assumed that LAI is constant and grass height is also constant.

On average, the isotope mass balance method contributes more flux to transpiration (13.6 % more) and HYDRUS-1D contributes more flux to soil evaporation (0.6 % more). Some studies (e.g. Herbst et al., 1996; Ferretti et al., 2003; Yepez et al., 2003; Robertson and Gazis, 2006; Roupsard et al., 2006; Xu et al., 2008; Wang et al., 2010; Wenninger et al., 2010; Zhang et al., 2011) including the FAO crop model calculated that the percentage of transpiration from total evaporation is more or less 70 %. The results from both isotope mass balance and HYDRUS-1D model are comparable which are 77.7 % and 64.1 % for isotope mass balance and HYDRUS-1D, respectively. In the mass balance method, interception evaporation and soil evaporation contribute almost equal to the total actual evaporation. This shows that the interception process plays a significant role.

4 Conclusions

To improve water use efficiency in agriculture especially in case of water scarcity, knowledge about water fluxes in the vadose zone is essential. The partitioning study can be used to separate the productive and unproductive fluxes. Two methods based on stable isotope technique and hydrometric measurements have been applied to quantify these fluxes and were compared. Both the isotope mass balance method and the HYDRUS-1D model show promising and comparable results.

Total evaporation calculated with isotopes and modeled do compare well with the results from the water balance method as a benchmark. Moreover, the isotope mass balance and the HYDRUS-1D model have the advantage that they enable to partition the evaporation flux into the productive (transpiration) and non-productive fluxes (soil evaporation and interception). Our findings show that, in terms of total evaporation flux, the isotope mass balance method is superior compared to the HYDRUS-1D model since this method has closer results to the water balance. Total evaporation from isotope mass balance is 237.3 mm (3.4 mm d^{-1}) and 243.1 mm (3.5 mm d^{-1}) from water balance. Total evaporation from HYDRUS-1D is slightly higher showing 256.2 mm (3.7 mm d^{-1}).

In contrast, in terms of high temporal resolution, the HYDRUS-1D model is better than the isotope mass balance. The partitioning results from the isotope mass balance are less reliable compared to the HYDRUS-1D model. In one segment, the isotope mass balance result shows high soil evaporation flux, and, in the other segment, isotope mass balance results show high transpiration flux. Moreover, the isotope mass balance method distributes more flux to transpiration than to soil evaporation, while the HYDRUS-1D model results are less. However, the portion of transpiration from both methods is acceptable (77.7 % from isotope mass balance and 64.1 % from HYDRUS-1D).

Both the isotope mass balance method and the HYDRUS-1D model show a great prospective to partition the evaporation fluxes for low temporal resolution and high temporal resolution. The temporal resolution is the main factor to consider which method is suitable. In general, we suggest to use the isotope mass balance method for low temporal resolution (e.g. monthly or seasonally) and the HYDRUS-1D model for high temporal resolution analysis (e.g. hourly or daily basis). This laboratory-scale experiment could give an insight for field-scale experiments. However, one should also measure percolation water and its isotopic composition and this is a significant limitation of this method for field applications. It is suggested to apply this experiment in the field during different climatic conditions especially during the spring season when plants will start to grow. Moreover, commodity plants are recommended to be used since this will give more benefits to the agricultural sector.

Acknowledgements. This study was carried out as a joint research between UNESCO-IHE, Delft, the Netherlands and IAEA isotope hydrology section, Vienna, Austria and financed by the Coordinated Research Project No 1429 (CRP 1429). The authors would like to thank the UNESCO-IHE laboratory staff for their great supports and also like to thank anonymous reviewers for their valuable comments to improve the manuscript.

Edited by: L. Wang

References

Allison, G. B.: The relationship between ^{18}O and deuterium in water in sand columns undergoing evaporation, J. Hydrol., 55, 163–169, 1982.

Barnes, C. J. and Turner, J. V.: Isotope exchange in soil water, in: Isotope tracers in catchment hydrology, Kendall and McDonnell, Elsevier, Amsterdam, 137–163, 1998.

Balazs, M. F., John, G. B., Pradeep, A., and Charles, J. V.: Application of isotope tracers in continental scale hydrological modeling, J. Hydrol., 330, 444-456, doi:10.1016/j.jhydrol.2006.04.029, 2006.

Brooks, J. R., Barnard, H. R., Coulombe, R., and McDonnell, J. J.: Ecohydrologic separation of water between trees and streams in a mediterranean climate, Nat. Geosci., 3, 100–104, 2010.

Calder, I. R., Narayanswamy, M. N., Srinivasalu, N. V., Darling, W. G., and Lardner, A. J.: Investigation into the use of deuterium as a tracer for measuring transpiration from eucalypts, J. Hydrol., 84, 345–351, 1986.

Calder, I. R.: Deuterium tracing for the estimation of transpiration from trees Part 2. Estimation of transpiration rates and transpiration parameters using a time-averaged deuterium tracing method, J. Hydrol., 130, 27–35, 1992.

Clark, I. and Fritz, P.: Environmental isotopes in hydrogeology, CRC Press, 1997.

Dansgaard, W.: Stable isotopes in precipitation, Tellus, 16, 436–468, 1964.

Dongmann, G., Nurnberg, H. W., Forstel, H., and Wagener, K.: On the enrichment of $H_2{}^{18}O$ in the leaves of transpiring plants, Rad. Environ. Biophys. 11, 41–52, 1974.

Ehleringer, J. R. and Dawson, T. E.: Water uptake by plants: perspectives from stable isotope composition, Plant, Cell Environ., 15, 1073–1082, 1992.

Feddes, R. A., Bresler, E., and Neuman, S. P.: Field test of a modified numerical model for water uptake by root systems, Water Resour. Res., 10, 1199–1206, 1974.

Feddes, R. A., Kowalik, P. J., and Zaradny, H.: Simulation of field water use and crop yield, John Wiley & Sons, New York, NY, 1978.

Feddes, R. A., Hoff, H., Bruen, M., Dawson, T., de Rosnay, P., Dirmeyer, P., Jackson, R. B., Kabat, P., Kleidon, A., Lilly, A., and Pitman, A.: Modeling root water uptake in hydrological and climate models, B. Am. Meteorol. Soc., 82, 2797–2809, December, 2001.

Ferretti, D. F., Pendall, E., Morgan, J. A., Nelson, J. A., LeCain, D., and Mosier, A. R.: Partitioning evapotranspiration fluxes from a Colorado grassland using stable isotopes: seasonal variations and ecosystem implications of elevated atmospheric CO_2, Plant Soil, 254, 291–303, 2003.

Gat, J. R.: Isotope hydrology a study of the water cycle, Imperial College Press, 2010.

Gehrels, J. C., Peeters, J. E. M., Vries, J. Jd., and Dekkers, M.: The mechanism of soil water movement as inferred from ^{18}O stable isotope studies, Hydrol. Sci. J., 43, 579–594, 1998.

Gerrits, A. M. J.: The role of interception in the hydrological cycle, PhD thesis, Delft University of Technology, The Netherlands, 2010.

Gerrits, A. M. J., Savenije, H. H. G., Hoffmann, L., and Pfister, L.: New technique to measure forest floor interception – an application in a beech forest in Luxembourg, Hydrol. Earth Syst. Sci., 11, 695–701, doi:10.5194/hess-11-695-2007, 2007.

Gerrits, A. M. J., Savenije, H. H. G., Veling, E. J. M., and Pfister, L.: Analytical derivation of the Budyko curve based on rainfall characteristics and a simple evaporation model, Water Resour. Res., 45, W04403, doi:10.1029/2008WR007308, 2009.

Gerrits, A. M. J., Pfister, L., and Savenije, H. H. G.: Spatial and temporal variability of canopy and forest floor interception in a beech forest, Hydrol. Process., 24, 3011–3025, doi:10.1002/hyp.7712, 2010.

Herbst, M., Kappen, L., Thamm, F., and Vanselow, R.: Simultaneous measurements of transpiration, soil evaporation and total evaporation in a maize field in northern Germany, J. Exp. Bot., 47, 1957–1962, 1996.

Kendall, C. and McDonnell, J. J.: Isotope tracers in catchment hydrology, Elsevier, Amsterdam, 1998.

Kirkham, M. B.: Principles of soil and plant water relations Elsevier, USA, 2005.

Koeniger, P., Leibundgut, C., Link, T., and Marshall, J. D.: Stable isotopes applied as water traces in column and field studies, Org. Geochem., 41, 31–40, doi:10.1016/j.orggeochem.2009.07.006, 2010.

Meissner, R., Rupp, H., Seeger, J., Ollesch, G., and Gee, G. W.: A comparison of water flux measurements: passive wick-samplers versus drainage lysimeters, Soil Sci., 61, 609–621, doi:10.1111/j.1365-2389.2010.01255.x, 2010.

Mook, W. G.: Environmental Isotopes in the Hydrological Cycle Principles and Applications UNESCO-IHP, Paris, 2000.

Riley, W. J., Still, C. J., Torn, M. S., and Berry, J. A.: A mechanistic model of $H_2{}^{18}O$ and $C^{18}OO$ fluxes between ecosystems and the atmosphere: model description and sensitivity analyses, Global Biogeochem. Cy., 16, 4241–4214, doi:10.1029/2002GB001878, 2002.

Robertson, J. A. and Gazis, C. A.: An oxygen isotope study of seasonal trends in soil water fluxes at two sites along a climate gradient in Washington state (USA), J. Hydrol., 328, 375–387, doi:10.1016/j.jhydrol.2005.12.031, 2006.

Rothfuss, Y., Biron, P., Braud, I., Canale, L., Durant, J.-L., Gaudet, J.-P., Richard, P., Vauclin, M., and Bariac, T.: Partitioning evapotranspiration fluxes into soil evaporation and plant transpiration using water stable isotopes under controlled conditions, Hydrol. Process, 3177–3194, doi:10.1002/hyp.7743, 2010.

Roupsard, O., Bonnefond, J.-M., Irvine, M., Berbigier, P., Nouvellon, Y., Dauzat, J., taga, S., Hamel, O., Jourdan, C., Saint-Andre, L., Mialet-Serra, I., Labouisse, J.-P., Epron, D., Joffre, R., Braconnier, S., Rouziere, A., Navarro, M., and Bouillet, J.-P.: Partitioning energy and evapo-transpiration above and below a tropical palm canopy, Agr. Forest Meteorol., 139, 252–268, doi:10.1016/j.agrformet.2006.07.006, 2006.

Rutter, A. J., Kershaw, K. A., Robins, P. C., and Morton, A. J.: A predictive model of rainfall interception in forests, 1. Derivation of the model from observations in a plantation of corsican pine, Agr. Meteorol., 9, 367–384, 1971.

Savenije, H. H. G.: The importance of interception and why we should delete the term evapotranspiration from our vocabulary, Hydrolog. Process., 18, 1507–1511, doi:10.1002/hyp.5563, 2004.

Simunek, J., Sejna, M., Saito, H., Sakai, M., and van Genuchten, M. T.: The HYDRUS 1D software package for simulating the one-dimensional movement of water, heat, and multiple solutes in variability-saturated media, University of California Riverside, California, 281 pp., 2008.

Sutanudjaja, E. H., van Beek, L. P. H., de Jong, S. M., van Geer, F. C., and Bierkens, M. F. P.: Large-scale groundwater modeling using global datasets: a test case for the Rhine-Meuse basin, Hydrol. Earth Syst. Sci., 15, 2913–2935, doi:10.5194/hess-15-2913-2011, 2011.

Tang, K. and Feng, X.: The effect of soil hydrology on the oxygen and hydrogen isotopic compositions of plants source water, Earth Planet. Sci. Lett., 185, 355–367, 2001.

van Genuchten, M. Th.: A numerical model for water and solute movement in and below the root zone. Research Report No 121, US Salinity laboratory, USDA, ARS, Riverside, California, 1987.

Wang, L., Caylor, K. K., Villegas, J. C., Barron-Gafford, G. A., Breshears, D. D., and Huxman, T. E.: Partitioning evapotranspiration across gradients of woody plant cover: Assessment of a stable isotope technique, Geophys. Res. Lett., 37, L09401, doi:10.1029/2010GL043228, 2010.

Wang, L., Good, S. P., Caylor, K. K., and Cernusak, L. A.: Direct quantification of leaf transpiration isotopic composition, Agr. Forest Meteorol., 154–155, 127–135, doi:10.1016/j.agrformet.2011.10.018, 2012a.

Wang, L., D'Odorico, P., Evans, J. P., Eldridge, D., McCabe, M. F., Caylor, K. K., and King, E. G.: Dryland ecohydrology and climate change: critical issues and technical advances, Hydrol. Earth Syst. Sci. Discuss., 9, 4777–4825, doi:10.5194/hessd-9-4777-2012, 2012b.

Wenninger, J., Beza, D. T., and Uhlenbrook, S.: Experimental investigations of water fluxes within the soil-vegetation-atmosphere system: stable isotope mass-balance approach to partition evaporation and transpiration, Phys. Chem. Earth, 35, 565–570, doi:10.1016/j.pce.2010.07.016, 2010.

Williams, D. G., Cable, W., Hultine, K., Hoedjes, J. C. B, Yepez, E. A., Simonneaux, V., Er-raki, S., Boulet, G., de Bruin, H. A. R., Chehbouni, A., Hartogensis, O. K., and Timouk, F.: Evapotranspiration components determined by stable isotope, sap flow and eddy covariance techniques, Agr.Forest Meteorol., 125, 241–258, doi:10.1016/j.agrformet.2004.04.008, 2004.

Xu, Z., Yang, H., Liu, F., An, S., Cui, J., Wang, Z., and Liu, S.: Partitioning evapotranspiration flux components in a subalpine shrubland based on stable isotopic measurements, Bot. Stud., 49, 351–361, 2008.

Yepez, E. A., Williams, D. G., Scott, R. L., and Lin, G.: Partitioning overstory and understory evapotranspiration in a semiarid savanna woodland from the isotopic composition of water vapor, Agr. Forest Meteorol., 119, 53–68, doi:10.1016/S0168-1923(03)00116-3, 2003.

Yepez, E. A., Huxman, T. E., Ignace, D. D., English, N. B., Weltzin, J. F., Castellanos, A. E., and Williams, D. G.: Dynamics of transpiration and evaporation following a moisture pulse in semiarid grassland: A chamber-based isotopes method for partitionong flux components, Agr. Forest Meteorol., 132, 359–276, doi:10.1016/j.agrformet.2005.09.006, 2005.

Zhang, S., Wen, X., Wang, J., Yu, G., and Sun, X.: The use of stable isotopes to partition evapotranspiration fluxes into evaporation and transpiration, Acta Ecologica Sinica, Elsevier, 30, 201–209, doi:10.1016/j.chnaes.2010.06.003, 2010.

Zhang, Y., Shen, Y., Sun, H., and Gates, J. B.: Evapotranspiration and its partitioning in an irrigated winter wheat field: A combined isotopic and micro meteorologic approach, J. Hydrol., 408, 203-211, doi:10.1016/j.jhydrol.2011.07.036, 2011.